12. SUPPLEMENTARY MATERIAL

12.1. TABLES

Table 1. Forward and reverse primers (5'→3') used to quantify mRNA of TLS polymerases.

Gene	Encoded protein	Starter	Sequence
PolH	DNA polymerase η	Forward	TCGAGGTATTGAACACGATCC
		Reverse	CCACGCGGTCATTATCATTTC
PolK	DNA polymerase κ	Forward	GCCTTGTACAGATGAGGTAG
		Reverse	AGTCTGTCAGTACTTCTCG
PolJ	DNA polymerase ι	Forward	CAGAAGTTAGGGACAGGAAATC
		Reverse	TTGAGAGGGACGTTAGGTAG
Rev1	DNA polymerase Rev1	Forward	GAAGGAATGGCTTCAGAGAG
		Reverse	TCCATCGGATCTGAGATAGTAG
PolZ	DNA polymerase ζ	Forward	CTAATCCTAGGCCAGTGAAAC
		Reverse	CGCTCAAGTATCTTAGAGACAG
Pgk1 (reference)	Phosphoglycerate kinase 1	Forward	CAAACAACCAAAGGATCAAGGC
		Reverse	ACAGAACATCCTTGCCCAGC
PpiA (reference)	Peptydyl-propyl isomerase A	Forward	AGACTGAATGGCTGGATGGC
		Reverse	TGGTTTGATGGGTAAAATGCC

Table 2. The oligodeoxynucleotides (5'→3') used as substrates for BER enzymatic assays.

Type of reaction	Sequence
Excision of 8-oxoG	CTGCAGCTGATGCGCC**(8-oxoG)**TACGGATCCCCGGGTAC
Excision of εA	CTGCAGCTGATGCGCCGT**(εA)**CGGATCCCCGGGTAC
Excision of U	CTGCAGCTGATGCGC**(U)**GTACGGATCCCCGGGTAC
Incision of AP-site	CTGCAGCTGATGCGC**(THF)**GTACGGATCCCCGGGTAC
Gap filling	CTGCAGCTGATGCGCCGT**(gap)**CGGATCCCCGGGTAC
Strand ligation	CTGCAGCTGATGCGC-**(nick)**-CGTACGGATCCCCGGGTAC
	Complementary
All	GTACCCGGGGATCCGTACGGCGCATCAGCTGCAG

12.2. FIGURES

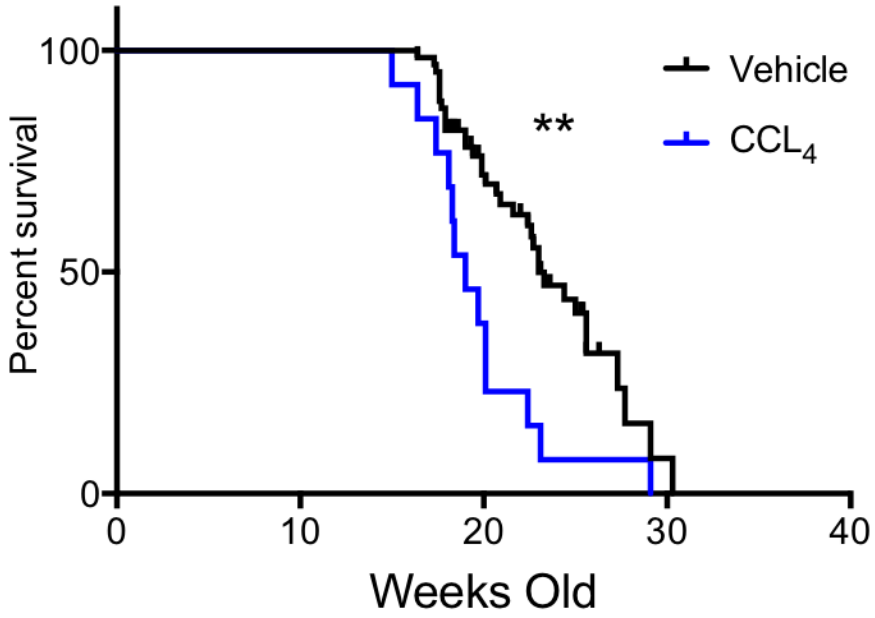

Fig. S1. Kaplain-Meier survival curve for *Ercc1*$^{-/\Delta}$ mice treated with CCl_4 vs. untreated (see also Fig. 2B). Mice were treated with 0.5 ml/kg CCl_4 1:1 sunflower oil twice per week for 5 weeks beginning at 10 weeks of age or the equivalent volume of vehicle only. The lipid peroxidation agent significantly shortened the lifespan of the DNA repair deficient mice (**p=0.0032, Log-rank (Mantel-Cox) test).

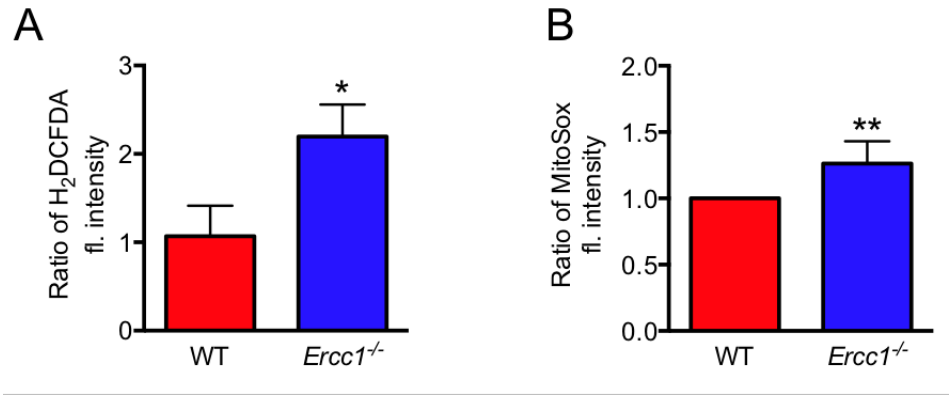

Fig. S2. Increased ROS in DNA repair-deficient *Ercc1*$^{-/-}$ primary MEFs. (A) DCFDA measured by flow cytometry were passage MEFs 5 grown at 20% O_2. H_2-DCFDA (C6827, Invitrogen, Carlsbad, CA) was used to measure general oxidative stress levels in primary WT and *Ercc1*$^{-/-}$ MEFs. 10mM H_2DCFDA in DMSO was diluted in PBS to a final concentration of 10 μM in PBS and added to cells in 10 cm dishes for 20 minutes at 37°C. Following incubation, cells were scraped, pelleted, and resuspended in 1 ml PBS. H_2DCFDA fluorescence intensity was measured on the Cyan LX 9 color high speed flow cytometer (Beckman Coulter, Brea, CA) and quantified using Summit v.4.3 software. (B) MitoSOX measured by flow cytometry. To measure superoxide anion levels, WT and *Ercc1*$^{-/-}$ MEFs were passage 5 grown at 3% O_2 in 10-cm dishes to 80-90% confluency and rinsed with PBS once. MitoSox reagent (M36008, Invitrogen, Carlsbad, CA) was diluted to a 2.5mM stock solution and applied to cells diluted 1:1000 in PBS for a 2.5 μM working solution. Cells were incubated for 20 minutes at 37°C and scraped, pelleted and resuspended in 1 ml PBS. MitoSox fluorescence intensity was acquired on the Cyan LX 9 color high speed flow cytometer (Beckman Coulter, Brea, CA) and quantified using Summit v.4.3 software. Fluorescence intensity of WT MEFs for each of 5 individual experiments was normalized to 1 and corresponding values for the *Ercc1*$^{-/-}$ MEF was plotted. Values are the mean of three separate experiments. Error bars represent ± SD. Statistical significance was determined by two-tailed unpaired Student's *t* test (*, $p<0.05$; **, $p<0.01$).

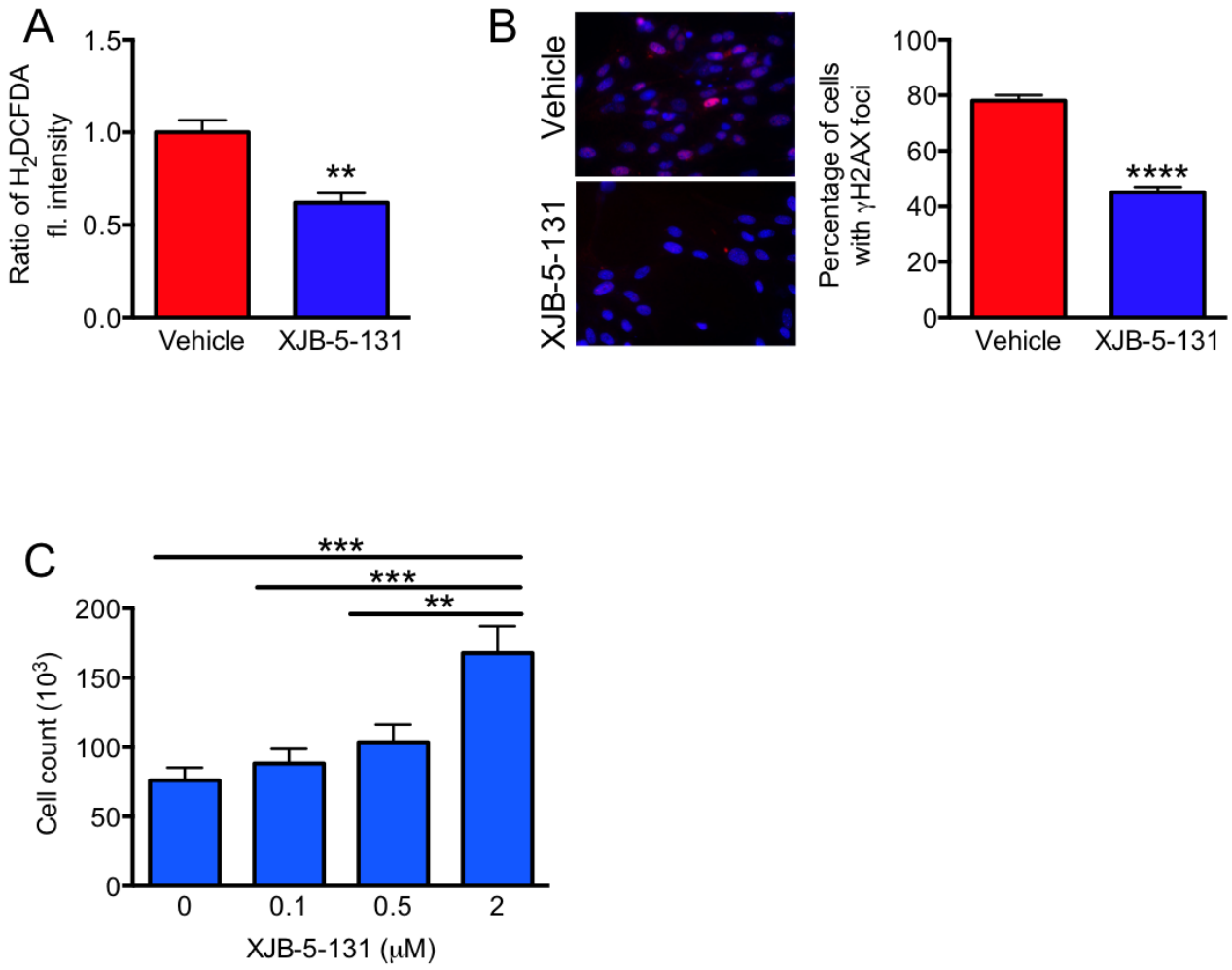

Fig. S3. XJB-5-131 suppresses ROS and signs of senescence. (A) DCFDA measured in p4-5 primary *Ercc1*$^{-/-}$ MEFs treated with the mitochondrial-targeted radical scavenger XJB-5-131 (0.5 μM) or DMSO vehicle only. (B) Immunodetection of γH2AX positive nuclei or cells. *Ercc1*$^{-/-}$ MEFs were cultured on glass coverslips until they reached 50% confluence. The cells were then treated with XJB-5-131 (0.5 μM) or vehicle only (DMSO). Forty-eight hours later, cells were fixed with 2% paraformaldehyde in PBS for 15 min, permeabilized with 0.1% Triton X-100 in PBS and stained for the phosphorylated form of H2AX detected with monoclonal anti-γ-H2AX (05-636, Millipore, Billerica, MA) and Alexa 594-conjugated goat anti-mouse IgG (A-11005, Invitrogen, Carlsbad, CA) in PBS with 0.15% glycine and 0.5% bovine serum albumin. γ-H2AX^{+} cells were counted with an Olympus BX51 fluorescent microscope. (C) *Ercc1*$^{-/-}$ MEFs were treated with various concentrations of XJB-5-131 or vehicle (indicated as 0) and cellular proliferation was quantified over 72 hours. Increased proliferation is consistent with decreased senescence. Values are the mean of three separate experiments. Error bars represent ± SD. Statistical significance was determined by two-tailed unpaired Student's *t* test or one-way ANOVA with Tukey's test (**, $p<0.01$; ***, $p<0.001$; ****, $p<0.0001$).

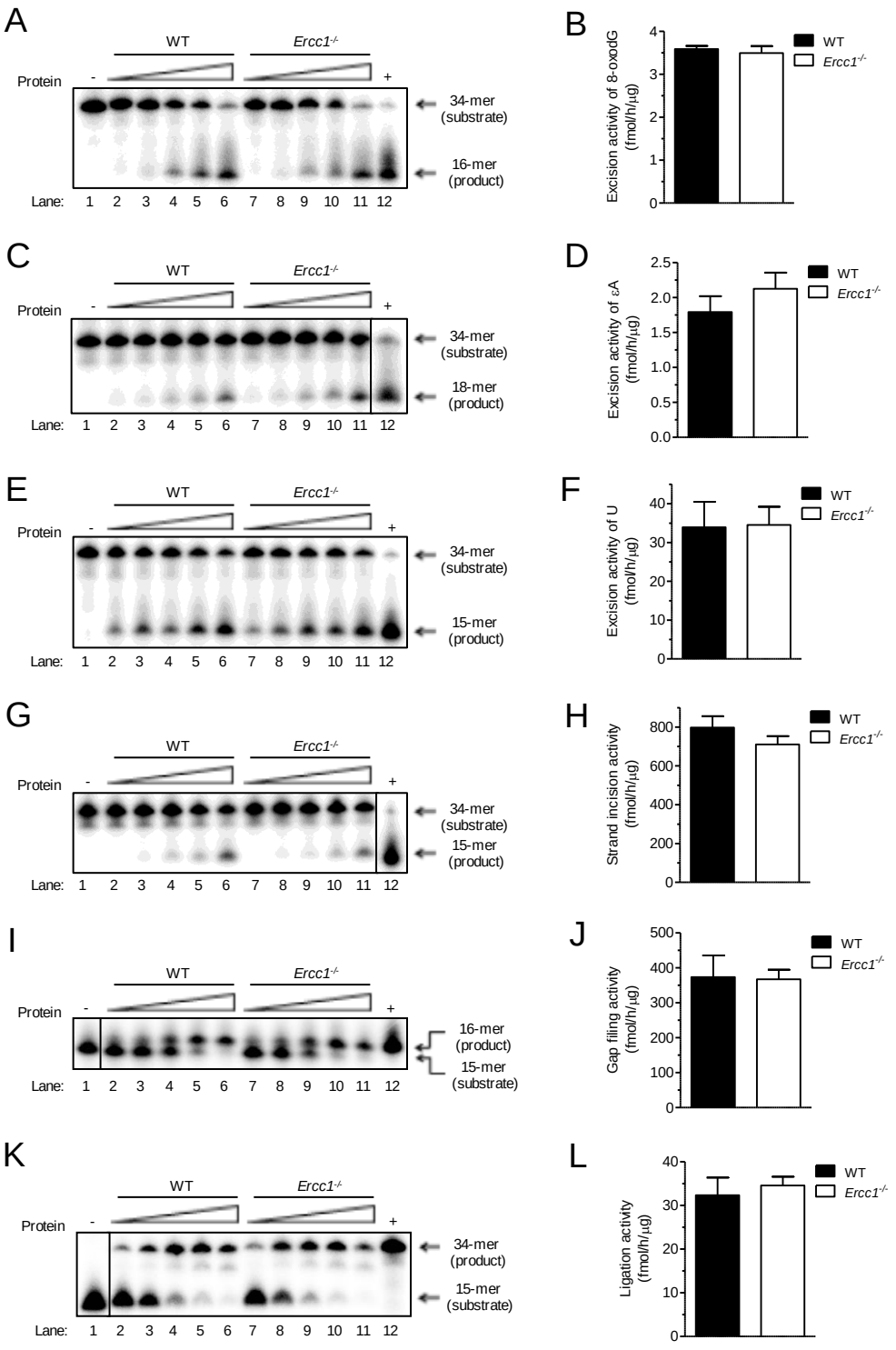

Fig. S4. Activities of base excision repair enzymes are not modified in *Ercc1*$^{-/-}$ MEFs. (A, C, E, G, I, K) PhosphorImages of representative gels showing: excision of 8-oxo-deoxyguanosine (A), ethenoadenine (C) and uracil (E), incision of AP-site (G), single-nucleotide gap filling (I) and ligation (K) by whole cell extracts from wild-type and *Ercc1*$^{-/-}$ immortalized MEFs. For excision activities radiolabeled double-strand oligodeoxynucleotides with a single lesion (8-oxodG, εA or

U) were used as substrates, while for incision activity – double-strand oligodeoxynucleotide with a tetrahydrofuran, an AP site analog. Gap filling was performed using double-strand oligodeoxynucleotides with 1-nt gap and ligation – using double-strand oligodeoxynucleotide with a nick. Reactions were run under the conditions described in Materials and Methods. (B, D, F, H, J, L) Quantitative analysis of data shown in A, C, E, G, I and K, respectively presented as a fmol of product per h per µg of protein. Values are the mean of three separate experiments. Error bars represent ± SD. No statistical significance was observed.

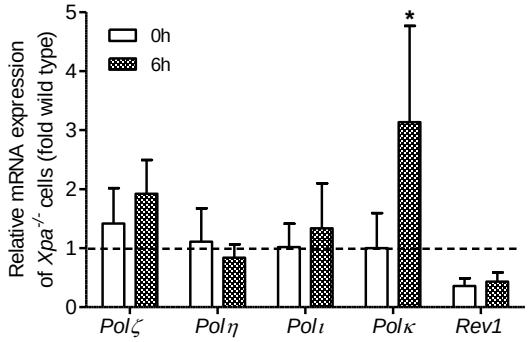

Fig. S5. Transcription of TLS polymerases in *Xpa*$^{-/-}$ MEFs. mRNA expression levels of TLS polymerases: Pol ζ, Pol η, Pol ι, Pol κ, Rev1 in *Xpa*$^{-/-}$ immortalized MEFs relative to WT control cells in response to HNE. mRNA levels were verified after 2 h of treatment with 20 µM HNE in serum-free medium followed by 4 h cell culture in fresh growth medium. Data are presented as a mean ± SD of at least three independent experiments. Statistical analysis was performed using Mann-Whitney *U*-test (*, $p<0.05$).

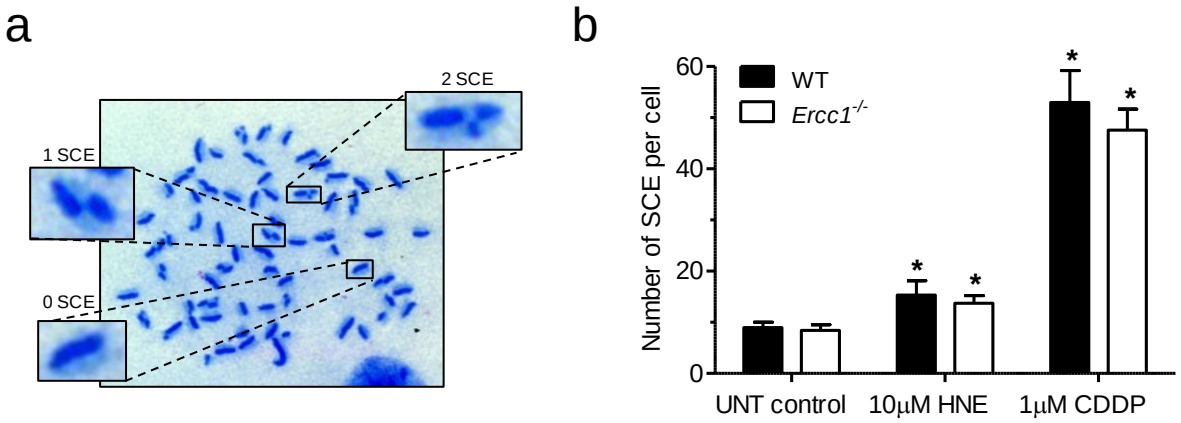

Fig. S6. HNE induces moderate increase in the frequency of SCEs at the same level in wild type and *Ercc1*$^{-/-}$ MEFs. Sister chromatid exchanges (SCEs) in cultured immortalized MEFs. Panel (A) shows representative metaphase plate of HNE-treated *Ercc1*$^{-/-}$ MEFs. Inserts show examples of individual chromosomes with or without sister chromatid exchanges. Chromosomes were stained with Fluorescence Plus Giemsa method and analyzed at 100× objective magnification. Different chromatid staining was obtained by incorporation of 5'-bromodeoxyuridine (BrdU) into chromosomal DNA for two cell cycles. (B) Sister chromatid exchange frequency in wild-type and

Ercc1$^{-/-}$ immortalized MEFs in response to 2 h treatment with 10 μM HNE or 1 μM cisplatin (CDDP) (positive control). Data bars are the mean ± SD of at least three independent experiments. Statistical analysis was done using Mann-Whitney *U*-test (*, $p<0.05$ *vs.* untreated control, unless otherwise indicated

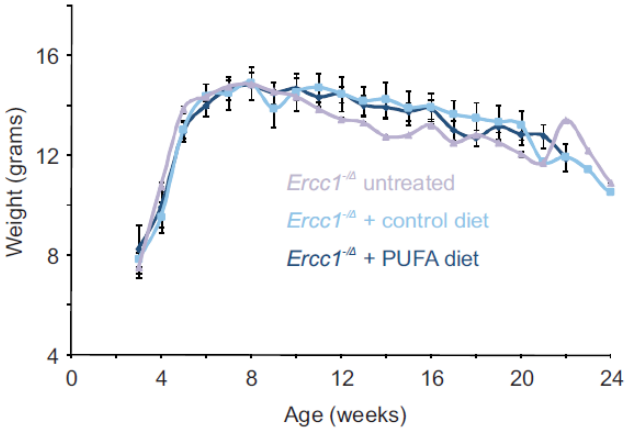

Fig. S7. Weight of *Ercc1*$^{-/\Delta}$ mice is not altered due to PUFA diet. Weights in grams of normal (light purple), control diet- (saturated fats, light blue), and PUFA diet-fed (dark blue) *Ercc1*$^{-/\Delta}$ mice starting at three weeks of age, when the mice were weaned onto the appropriate diet, until death.

12.3. DISCUSSION

The observation that *Ercc1*$^{-/-}$ MEFs are less susceptible to ACR than other LPO products (Fig. 1) might be explained by the existence of a backup repair system more specific for ACR adducts *E. coli* AlkB dioxygenase (EcAlkB) can oxidatively dealkylate ACR and MDA adducts in ssDNA, however with different efficiency. ACR adduct to Gua, γ-OH-PdG is very toxic because it can form intra- and inter-strand crosslinks. It was repaired by EcAlkB most efficiently, followed by the MDA adduct M1dG, and another ACR adduct isomer, α-OH-PdG, which is unable to form crosslinks, but inhibits human DNA polymerases and induces mutations [1]. Since the mammalian AlkB homolog, ALKBH2, belongs to the same structural family as EcAlkB [2] its activity may be similar. Interestingly AlkB-mediated repair of ACR and MDA adducts was less efficient in dsDNA [1].

SCE are large chromatid rearrangements commonly induced by DNA ICLs [3]. Formation of SCEs in response to ICLs requires unhooking of the ICL by ERCC1-XPF, followed by homologous

recombination-mediated repair of the collapsed replication fork [4]. Since LPO products are implicated in forming ICLs, and we demonstrated increased LPO in ERCC1-deficient mice (Fig. 2C) and HNE-treated cells (Fig. 3D, C), we measured SCEs in response to HNE and the known crosslinking agent cisplatin. In untreated cells, the number of SCEs was similar in WT and *Ercc1*$^{-/-}$ cells (Fig. S3). After treatment with 10 μM HNE, the number of SCEs in both cell lines increased, consistent with HNE inducing ICLs. Cisplatin induced significantly more SCEs than HNE. The observation that SCE levels were similar if slightly lower in *Ercc1*$^{-/-}$ cells compared to WT is consistent with earlier reports [5].

12.4. REFERENCES

1. Singh, V., et al., Mechanism of Repair of Acrolein- and Malondialdehyde-Derived Exocyclic Guanine Adducts by the alpha-Ketoglutarate/Fe(II) Dioxygenase AlkB. Chemical Research in Toxicology, 2014. 27(9): p. 1619-1631.

2. van den Born, E., et al., Bioinformatics and functional analysis define four distinct groups of AlkB DNA-dioxygenases in bacteria. Nucleic Acids Res, 2009. 37(21): p. 7124-36.

3. Kano, Y. and Y. Fujiwara, Roles of DNA interstrand crosslinking and its repair in the induction of sister-chromatid exchange and a higher induction in Fanconi's anemia cells. Mutat Res, 1981. 81(3): p. 365-75.

4. Clauson, C., O.D. Scharer, and L. Niedernhofer, Advances in understanding the complex mechanisms of DNA interstrand cross-link repair. Cold Spring Harb Perspect Biol, 2013. 5(10): p. a012732.

5. Niedernhofer, L.J., et al., The structure-specific endonuclease Ercc1-Xpf is required to resolve DNA interstrand cross-link-induced double-strand breaks. Mol Cell Biol, 2004. 24(13): p. 5776-87.